COMMUNICATIONS IN NUMERICAL METHODS IN ENGINEERING, Vol. 11, 887–897 (1995)

hp-VERSION FINITE ELEMENTS FOR GEOMETRICALLY NON-LINEAR PROBLEMS

ROLAND KRAUSE, ROLAND MÜCKE* AND ERNST RANK
Numerische Methoden und Informationsverarbeitung, FB Bauwesen, University of Dortmund, Germany

SUMMARY

A *p*-version of the finite element method and an *hp*-extension is applied to a geometrically non-linear model problem. Starting from a standard formulation in finite elasticity, some implementation details are outlined. The robustness and efficiency of this method, as already well known for linear problems, is demonstrated. In two numerical examples high accuracy and exponential rate of convergence in energy are shown. The method presented can be used effectively in problems where standard low-order plane strain elements fail to give accurate results.

KEY WORDS geometrically non-linear problem; finite elasticity; *p*-version; *hp*-extension

1. INTRODUCTION

In contrast to the *h*-version of the finite element method, where convergence is achieved by successive (uniform or adaptively controlled) mesh refinement, the *p*-version keeps the mesh fixed and increases (uniformly or selectively) the polynomial degree of the element's shape functions. In an *hp*-version, mesh refinement and increase of the polynomial degree are combined in a powerful method to achieve highly accurate results.

p- and *hp*-versions have proven to be attractive alternatives to the standard *h*-version for a variety of problems in computational mechanics, like plane elasticity,[1,2] plate problems[3] as well as for incompressible flow problems.[4] Some of the most interesting features of *p*- and *hp*-extensions are the following:

- *p*-version approximation on graded meshes has proven to give very accurate results. For linear elliptic boundary value problems it was shown[5] that the *p*-extension has an exponentially converging preasymptotic range and that an *hp*-extension provides even asymptotic exponential convergence in energy norm.
- *p*-version implementations apply hierarchical shape functions in a very natural way. Therefore a higher-order reanalysis need not recompute the whole system matrix but can use the results of the analysis before on the element level as well as on the system level.
- Higher-order shape functions are very robust against geometric distortion and a high aspect

* Present address: ABB Corporate Research, CH-5405 Baden-Dättwil, Switzerland.

CCC 1069-8299/95/110887–11
© 1995 by John Wiley & Sons, Ltd.
Received 9 May 1994
Revised 1 March 1995

In our first example, a Mode I fracture problem is considered. In Reference 12 this example was used to verify numerically that the order of singularity in the non-linear case is similar to that in the linear case. In this Reference convergence orders for uniform and adaptive h-versions in energy were investigated. In addition to the above, we are here concerned with the p- and hp-extensions for the same problem. An elastic plate of thickness 1, with uniform tension load and cracks as shown in Figure 1, was computed with the p-version FE-Code. Plane strain conditions and a Poisson ratio of $\nu = 0{\cdot}3$ is assumed, and the elasticity modulus is set to $E = 1{\cdot}0 \times 10^5$. Symmetry boundary conditions permit investigation of only one-quarter of the domain.

Uniform meshes varying in density from $h = a/2$ up to $h = a/28$ and meshes with different grading at the crack tip have been constructed to investigate h- and p-version extensions. One graded mesh, with a geometric refinement towards the crack tip, is shown in Figure 2. The significant difference between linear and geometrically non-linear solution of this problem is shown best in the load-displacement curve (Figure 3) for the crack opening point A in Figure 1. Here the vertical displacement differs by a factor of 2·8.

From an extrapolation of the results of p-version computations with $p = 6, 7, 8$, we estimate the energy of the exact solution for the geometrically non-linear crack problem to be

$$U(u_{EX}) = 5{\cdot}38994 \times 10^6 \tag{18}$$

Now we are able to define a relative error in an energy measure (which is, due to the non-linearity of the problem, *no norm*) by

$$(e_r)_E = \sqrt{\frac{U(u_{EX}) - U(u_{FE})}{U(u_{EX})}} \times 100\% \tag{19}$$

and to plot the $\log(e_r)_E$ against $\log(N)$ curves.

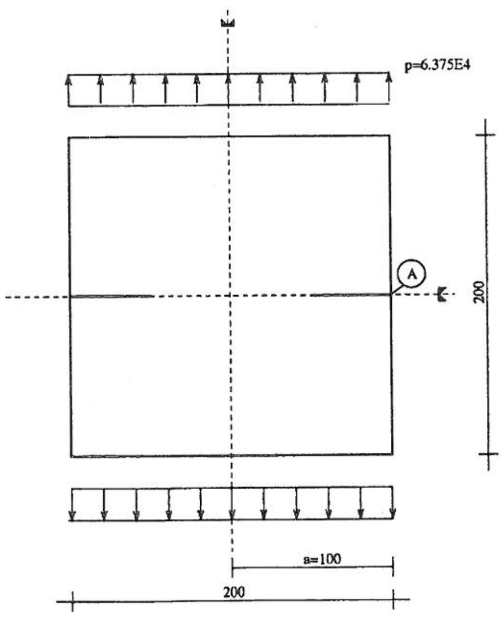

Figure 1. Crack problem

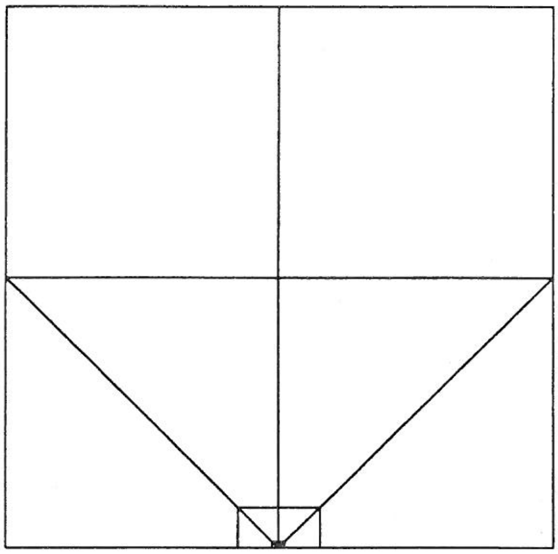

Figure 2. Example for a graded mesh

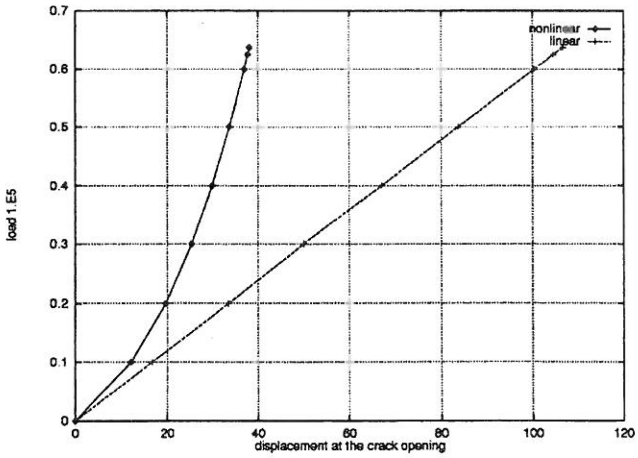

Figure 3. Load displacement curves

Figure 4 shows the convergence curves for various extension processes. First comparing h- and p-versions on uniform meshes (the two upper curves in Figure 4) shows a behaviour that was also observed in the linear case. The convergence rate of the h-extension is half that of the p-extension, both curves being asymptotically straight lines with a constant slope controlled by the strength of the singularity. Higher accuracy can hardly be obtained by either of these two extensions. The lower three curves show p-extensions on three graded meshes with a common geometric progression factor of $r = 0{\cdot}15$ and one, two and three layers of refinement at the crack tip. As expected from linear theory, we observe an inverted S-shape of the curves, demonstrating an exponential preasymptotic range of convergence and a slowing to the asymptotic range of algebraic convergence. It can be seen that a graded mesh with 16 elements and only three layers of refinement allows us to achieve a relative error in the energy measure of about 5 per cent with less than 200 degrees of freedom (d.o.f.). A comparison to an adaptive h-version shows the dramatic improvement of the hp-approach. Extrapolating from the results in Reference 12 (linear triangular elements, adaptive refinement), a level of 5 per cent in the error measure as defined in (19) needs more than 3500 d.o.f. An accuracy of 1·4 per cent, which is achieved in the hp-approach just by using the same mesh and increasing the polynomial order to $p = 4$ (288 d.o.f.) could only be obtained with more than 100,000 degrees of freedom in an adaptive h-version!

Another interesting aspect of this example was that the number of corrector iterations of Newton's method was not affected by the choice of the polynomial degree of our FE approximation. In all computations and in each load increment the quadratic convergence of Newton's method could be observed.

In the second example we consider a typical situation where already for moderately high load levels a geometrically non-linear computation is necessary. For planar problems such behaviour is observed especially when long and beam-like structures are part of the elastic body. As it is well known that low-order plane elements are very inaccurate in this situation, a commonly used

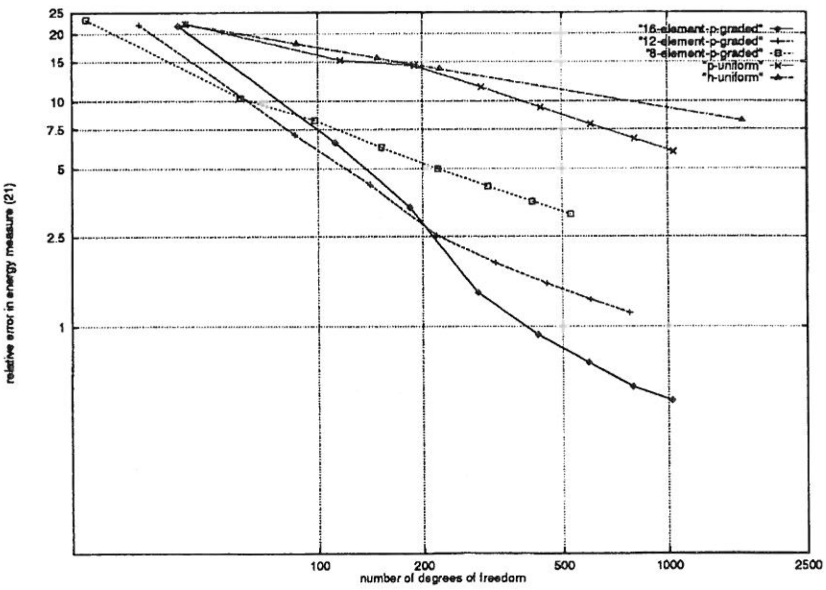

Figure 4. p-version on graded meshes

technique is to couple one-dimensional beam elements to the two-dimensional plane elements. Although this method allows a simple modelling of the geometrically non-linear effects, it is not possible to study stress concentrations in the transition range of the 1D- to the 2D-structure. Nevertheless, this is the point the design engineer is most interested in. Only sophisticated models like 'dimensional adaptivity'[13] allow a consistent discretization of the non-linearity and the singular solution behaviour as well. We show here that the p-method presented gives a simple and very accurate method of computation for this problem without changing the dimension of the model.

Geometry and boundary conditions for the structure, an electrical contact switch, are shown in Figure 5. The structure is loaded by a horizontal and a vertical tension at the left boundary of the head. The mesh is refined with three layers of elements at the upper re-entrant corners and at the clamped edge at the switch's bottom. A zoomed plot of the mesh at the transition between head structure and body is given in Figure 6.

Results of a p-extension on this graded mesh are now compared to an h-approximation on the refined mesh of Figure 7, computed with quadratic elements and 6836 degrees of freedom in the standard finite element code ABAQUS.[14]

Figure 8 shows load-displacement curves at point 1 of Figure 5 for linear and non-linear analyses for $p=3$ on the graded mesh and for the ABAQUS reference solution. Firstly, it can be seen that the linear solution of $p=8$ differs completely from the non-linear results. Considering the solutions for the non-linear computation, the load-displacement curve for $p=3$ could not be distinguished visually from that of $p=8$. Using the $p=8$ computation as a reference solution, the displacement error for $p=3$ with 676 d..f. is only 1·2 per cent, whereas the ABAQUS-solution, with more than ten times the number of degrees of freedom, shows a displacement error of about 2·5 per cent.

As the homogeneous solution of the beam is a polynomial of third degree, good results could, of course, be expected for $p=3$. Yet this example demonstrates how p-elements perform well in non-linear analysis even when having a very large aspect ratio. Here only four p-elements at negligible computational cost were able to model the behaviour of the beam. The

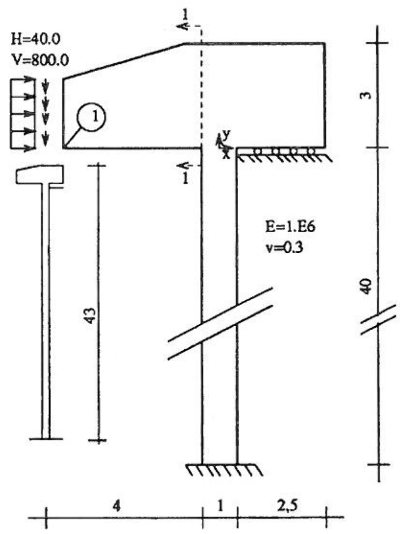

Figure 5. Electrical switch, geometry and boundary conditions

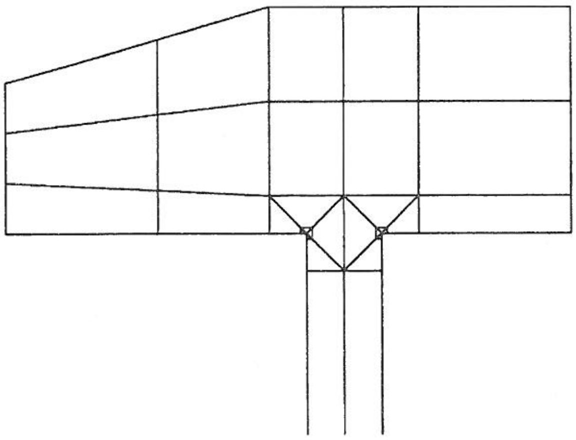

Figure 6. Transition with refined mesh

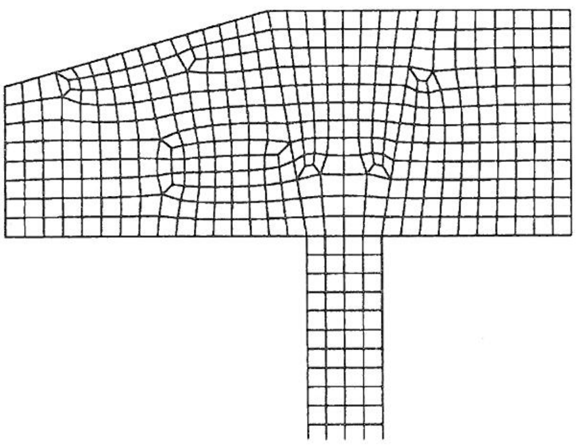

Figure 7. Part of *h*-version mesh, quadratic elements, 6836 d.o.f.s for ABAQUS reference solution

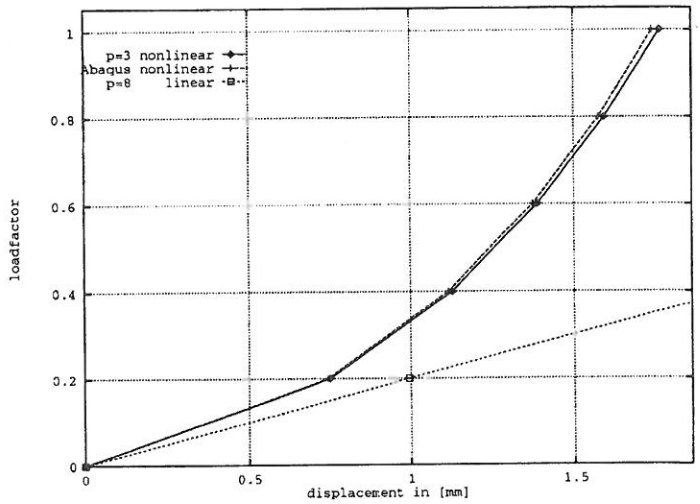

Figure 8. Load displacement curves

Table I. Stresses at $x=-0{\cdot}4758$ and $y=0{\cdot}00065$ with $r=0{\cdot}025$

		Linear			Nonlinear		
p	N	σ_x	σ_y	τ_{xy}	σ_x	σ_y	τ_{xy}
1	176	−8608	−11900	4721	−8703	−12042	4789
2	411	−11356	−10698	3469	−7533	−5144	2180
3	676	−11639	−9885	3716	−6300	−3308	2135
4	1059	−10725	−10394	3564	−5911	−3405	2136
5	1560	−10855	−10388	3228	−6113	−3419	1833
6	2179	−10786	−10379	3161	−6092	−3413	1819
7	2916	−10876	−10385	3102	−6194	−3414	1760
8	3771	−10880	−10380	3091	−6202	−3418	1759

advantage of using the same mechanical model instead of a coupling of beam elements to a 2D model becomes even more evident when considering the singular points at the re-entrant corners of the structure. A common 'economic' computation would have solved the beam problem and then made another computation necessary to obtain stresses at these points of interest. As the p-extension uses the same model in the whole domain, stresses and strain are immediately available.

Results are given in Table I. Stresses at the point with co-ordinates $x=-0{\cdot}4758$ and $y=0{\cdot}0065$ corresponding to a distance of $r=0{\cdot}025$ to the re-entrant corner are compared, p again varying from 1 to 8. Although very close to the singular point, excellent convergence is observed in both the linear and the non-linear cases.

4. CONCLUSIONS

In advanced engineering the study of non-linear effects is becoming more and more part of the business. The non-linear computational analysis, however, requires a much higher evaluation effort as in the corresponding linear situation. In view of this, it is very necessary to optimize the finite element approximation in such a way that a certain limit of the discretization error can be achieved with the lowest possible number of degrees of freedom.

In linear analysis it turns out that often the *hp*-version finite elements approach this challenge best. We have discussed in this paper the main features of an *hp*-version for a geometrically non-linear model problem. It could be shown numerically that the advantages of the high convergence rate of the *p*-approximation on graded meshes survive in the investigated non-linear situation.

Of course, large displacement type non-linearities cover only a small range of the models applied in advanced engineering. In view of this, the work at hand is only a first step to treating more complex situations with *hp*-version elements.

ACKNOWLEDGEMENT

The work of R. Mücke was supported by the Alexander von Humboldt Foundation.

REFERENCES

1. I. Babuška and B. Szabó, 'On the rates of convergence of the finite element method', *Int. j. numer. methods eng.*,**18**, 323–341 (1982).
2. E. Rank and I. Babuška, 'An expert system for the optimal mesh design in the *hp*-version of the finite element method', *Int. j. numer. methods eng.*, **24**, 2087–2106 (1987).
3. S. Holzer, E. Rank and H. Werner, 'An implementation of the *hp*-version of the finite element method for Reissner–Mindlin plate problems', *Int. j. numer. methods eng.*, **30**, 459–471 (1990).
4. J. T. Oden, L. Demkowicz, T. Strouboulis and Ph. Devloo, 'Adaptive methods for problems in solid and fluid mechanics, in Babuška, Zienkiewicz, Gago, Oliviera, (Eds.), *Accuracy Estimates and Adaptive Refinements in Finite Element Computations*, Wiley, 1986, pp. 249–280.
5. W. Gui and I. Babuška, 'The h, p, and $h-p$ versions of the finite element method in 1 dimension. Part 1: The error analysis of the p-version', *Numer. Math.*, **49**, 577–612 (1986); Part 2: The error analysis of the h- and $h-p$ versions, *Numer. Math.*, **49**, 659–683 (1986).
6. B. Szabó and I. Babuška, *Finite Element Analysis*, Wiley, 1990.
7. I. Babuška and E. Rank, 'An expert-system-like feedback approach in the *hp*-version of the finite element method', *Finite Elem. Anal. Des.*, **3**, 127–147 (1987).
8. E. Rank, 'Adaptivity and accuracy estimation for FEM and BIEM, Chapter 1 in Brebbia and Aliabadi (Eds.), *Adaptive Finite and Boundary Element Methods*, Comp. Mech. Publications, Southampton, Boston, 1993.
9. S. Holzer and Z. Yosibash, 'The *p*-version of the finite element method in incremental elasto-plastic analysis', Report, Center for Computational Mechanics, Washington University, St. Louis, MO 63130, December 1993.
10. M. A. Crisfield, 'Non-linear finite element analysis of solids and structures', Vol. 1, Wiley, 1991.
11. H. R. Schwarz, *Methode der finiten Elemente*, Teubner Studienbücher, Stuttgart, 1980.
12. R. Mücke and J. R. Whiteman, 'On the a-posteriori error estimate of finite element solutions for finite elasticity', *Int. j. numer. methods eng.*, to be published.
13. E. Stein and S. Ohnimus, 'Dimensions-Adaptivität bei Finite-Element-Berechnungen von Stäben und Platten', *Z. Angew. Math. Mech.*, **73**, (6), (1993).
14. ABAQUS theory manual 5.4, Hibbitt, Karlson & Sorensen Inc., 1994.
15. B. Szabó, 'Mesh design for the *p*-version of the finite element method', *Comput. Methods Appl. Mech. Eng.*, **55**, 181–197 (1986).

ratio of the elements chosen. Therefore they can readily be used to model structures of very different inherent dimensions, like plane structures being degenerated to beam-like structures in some parts.

- Due to the 'richness' of the higher-order element spaces the notorious problem of locking, e.g. in Reissner–Mindlin-plate problems, disappears for polynomial degrees of four or higher in a p-approximation.[3]
- For a rather wide class of elliptic problems,[6,7] rules for an a priori mesh construction are known, making it possible to achieve a desired accuracy in one step with only minor additional analysis before the construction of the mesh and the assignment of a necessary polynomial degree.
- Adaptive control of an *hp*-extension can also make use of these a priori rules, refining a finite element mesh only near singular points of the exact solution.[8]

Although most of the results in p- and *hp*-analysis have been achieved for linear problems, all the features mentioned above would be even more attractive for non-linear computations. Yet only recently a p-version for an incremental elasto–plastic problem has been considered.[9] The goal of this paper is to investigate p- and *hp*-extensions for another non-linear model problem, namely plane elasticity in a geometrically non-linear formulation. After a short outline of the model in Section 2, we present a brief survey on our p-implementation. Section 3 gives a discussion of numerical examples, demonstrating the exponential rate of convergence in energy, the very high accuracy in displacements and stress resultants as well as the robustness of the method.

2. GOVERNING EQUATIONS AND IMPLEMENTATION

Following the notation of Reference 10, we consider the general physical principle of virtual work expressed by

$$\delta\Pi(\mathbf{u}) = \delta W_i(\mathbf{u}) + \delta W_a(\mathbf{u}) = \int_\Omega \mathbf{S}_2 : \delta\mathbf{E}_2 \, \mathrm{d}\Omega - \int_\Omega \bar{\mathbf{p}} \cdot \delta\mathbf{u} \, \mathrm{d}\Omega - \int_{\Gamma_q} \bar{\mathbf{q}} \cdot \delta\mathbf{u} \, \mathrm{d}\Gamma \tag{1}$$

Here, $\delta\Pi(\mathbf{u})$ denotes the variation of the total potential energy of the mechanical system and $\delta W_i(\mathbf{u})$ and $\delta W_a(\mathbf{u})$ are the variations of the internal virtual energy and the external virtual work of the body force $\bar{\mathbf{p}}$ and the surface force $\bar{\mathbf{q}}$, respectively. With $\Omega \subset \mathrm{R}^n$, $n = 1, 2, 3$ we denote the domain in its reference configuration and $\Gamma = \partial\Omega$ is its boundary. On Γ either the displacement is prescribed, $\mathbf{u} = \bar{\mathbf{u}}$ on Γ_u, or the surface load, $\mathbf{q} = \bar{\mathbf{q}}$ on Γ_q, must be given; $\Gamma = \Gamma_u \cup \Gamma_q$, $\Gamma_u \cap \Gamma_q = \varnothing$. The internal energy is characterized by the double scalar product of the 2nd Piola stress tensor $\mathbf{S}_2$ and the Green strain tensor $\mathbf{E}_2$. They can also be given by their vector representations (here for the case of two-dimensional formulations):

$$\mathbf{S}^{\mathrm{T}} = [S_{xx} \; S_{yy} \; S_{xy}] \tag{2}$$

$$\mathbf{E}^{\mathrm{T}} = [E_{xx} \; E_{yy} \; E_{xy}] \tag{3}$$

Using the deformation gradient $\mathbf{F}$ defined by

$$\mathrm{d}\mathbf{x} = \mathbf{F}\,\mathrm{d}\mathbf{X} = \begin{bmatrix} 1 + u_{,x} & u_{,y} \\ v_{,x} & 1 + v_{,y} \end{bmatrix} \begin{bmatrix} \mathrm{d}X \\ \mathrm{d}Y \end{bmatrix} \tag{4}$$

where $\mathrm{d}\mathbf{x}$ and $\mathrm{d}\mathbf{X}$ are infinitesimal line elements of the deformed configuration and the reference configuration, respectively, and $u_{,x} = \partial u/\partial x$, the 2nd Piola stresses can be transformed into the true Cauchy stresses (force by unit area of the deformed configuration),

$$\tau = \frac{1}{\det(\mathbf{F})} \mathbf{FSF}^{\mathrm{T}} \tag{5}$$

or the first Piola stresses (force per unit area of the undeformed configuration),

$$\mathbf{P} = \mathbf{FS} \tag{6}$$

The relationship between the Green strain and the displacement is given by

$$\mathbf{E}_2 = \tfrac{1}{2}(\mathbf{F}^{\mathrm{T}}\mathbf{F} - \mathbf{I}_2) \tag{7}$$

where $\mathbf{I}_2$ denotes the unit tensor of second order. After some manipulations we obtain

$$\mathbf{E} = \mathbf{E}_l + \mathbf{E}_{nl} = [\mathbf{H} + \tfrac{1}{2}\mathbf{A}(\theta)]\theta \tag{8}$$

$$= \left\{ \begin{bmatrix} 1 & 0 & 0 & 0 \\ 0 & 0 & 0 & 1 \\ 0 & 1 & 1 & 0 \end{bmatrix} + \frac{1}{2} \begin{bmatrix} u_{,x} & 0 & v_{,x} & 0 \\ 0 & u_{,y} & 0 & v_{,y} \\ u_{,y} & u_{,x} & v_{,y} & v_{,x} \end{bmatrix} \right\} \begin{bmatrix} u_{,x} \\ u_{,y} \\ v_{,x} \\ v_{,y} \end{bmatrix} \tag{9}$$

and

$$\delta\mathbf{E} = [\mathbf{H} + \mathbf{A}(\theta)]\delta\theta \tag{10}$$

Note that the Green strain can be interpreted as the sum of the linear strain $\mathbf{E}_l$ and a non-linear part $\mathbf{E}_{nl}$.

The relation between the stresses and strains are described by a constitutive law. In the most simple case we can assume a linear relation given by

$$\mathbf{S}_2 = \mathbf{C}_4 : \mathbf{E}_2 \tag{11}$$

or in matrix representation by

$$\mathbf{S} = \mathbf{CE} \tag{12}$$

where $\mathbf{C}_4$ is the Hooke tensor of fourth order and $\mathbf{C}$ is the corresponding Hooke matrix.

The finite element discretization can be based on the variational formulation (1) of the boundary value problem. Using the finite element approximation

$$\bar{\mathbf{u}} = \sum_i N_i a_i, \qquad i = 1, \ldots, n \tag{13}$$

where N_i are shape functions and a_i are the unknown parameters, the continuous problem is turned into a finite set of non-linear algebraic equations of the form

$$\mathbf{K}(\mathbf{a})\mathbf{a} - \mathbf{f} = \mathbf{0} \tag{14}$$

Here, $\mathbf{a}$ denotes the vector of unknown parameters, $\mathbf{K}(\mathbf{a})$ is the non-linear stiffness matrix and $\mathbf{f}$ is the load vector.

In our implementation the solution of the non-linear system (14) is achieved using an incremental fully Newton–Raphson method as described, for example, in Reference 10. We assume that the non-linear system is solved accurately enough so that only the discretization error needs to be considered subsequently.

The main characteristics of the stiffness matrix $\mathbf{K}(\mathbf{a})$ are correlated to the applied p-version functions. General techniques to be used for an efficient implementation of p-elements are described in Reference 6; an effective data structure is outlined, for example, in Reference 8. Therefore only two main principles important for this study are discussed.

Following Reference 6, our p-version implementation uses hierarchical basis functions, which can easily be implemented up to any desired polynomial degree. Starting with the two linear shape functions on a standard element $[-1, +1]$, a whole family of shape functions in one space dimension is obtained by definition of a sequence of polynomials P_i with degree i, vanishing at the end points of the standard element.

A possible choice for P_i is given by integrals of the Legendre polynomials defined by

$$P_i(\zeta) = \int_{t=-1}^{\zeta} L_{i-1}(t)\,\mathrm{d}t$$

with

$$L_n(x) = \frac{1}{2^{n-1}(n-1)!}\,\frac{\mathrm{d}^n(x^2-1)^n}{\mathrm{d}x^n} \quad \text{for} \quad n \geqslant 1 \tag{15}$$

A construction of a hierarchical family of two-dimensional (and similarly three-dimensional) elements is now quite straightforward. Standard shape functions are defined on a standard square $[-1, 1] \times [-1, 1]$ in local co-ordinates ζ, η as tensor products of the one-dimensional shape functions. They can be grouped into three classes. Elements in the first group are called basic modes, being the 'usual' bilinear shape functions. The second class are edge modes. Hierarchical modes for edge $\eta = 1$ (and analogously for the other edges of the standard element) are defined by

$$H_i(\zeta, \eta) \coloneqq P_i(\zeta)(\eta + 1)/2 \tag{16}$$

Edge modes are identically zero on all edges except on their defining edge. The third class are bubble modes, being given by

$$H_{kl}(\zeta, \eta) = P_k(\zeta)P_l(\eta), \qquad k, l \geqslant 2 \tag{17}$$

and disappearing on all edges of the element.

Although this classification offers a systematic way to an implementation of variable-degree shape functions in different parts of the mesh (each element is by construction a 'transition element'), we are using for simplicity only a uniform polynomial degree over the entire mesh in this study.

Because of the hierarchical nature of the shape functions, the resulting (sparse) equation system has in general large bandwidth, making common direct solvers unsuitable. Therefore, in our implementation a cg-solver with ILU-preconditioning[11] in a sparse storage scheme is used, being embedded into the Newton–Raphson method for the solution of the non-linear equations.

3. NUMERICAL EXAMPLES

Our aim in this Section is to show that performance and convergence rates of the p-version for the given geometrically non-linear problem are very similar to that known from linear elasticity. It will be seen that, as in the linear case, the quality of the p-version strongly depends on the mesh design.